A Novel Rheometer Design for Yield Stress Fluids

Joseph R. Samaniuk, Timothy W. Shay, Thatcher W. Root, and Daniel J. Klingenberg
Dept. of Chemical and Biological Engineering, University of Wisconsin-Madison, Madison, WI 53706

C. Tim Scott
USDA Forest Service, Madison, WI 53726

DOI 10.1002/aic.14329
Published online January 3, 2014 in Wiley Online Library (wileyonlinelibrary.com)

An inexpensive, rapid method for measuring the rheological properties of yield stress fluids is described and tested. The method uses an auger that does not rotate during measurements, and avoids material and instrument-related difficulties, for example, wall slip and the presence of large particles, associated with yield stress fluids. The method can be used for many types of yield stress fluids, including concentrated lignocellulosic biomass. Sample preparation prior to measurement is minimal, reducing, or eliminating disruption of the sample. We show that measurements using this technique compare well with measurements obtained with a vane rheometer. A variation of the described method is proposed that would make it easier to measure time-dependent rheological properties. © 2014 American Institute of Chemical Engineers *AIChE J*, 60: 1523–1528, 2014
Keywords: rheometer, rheology, auger, yield stress, lignocellulosic biomass

Introduction

Lignocellulosic biomass can be converted to fuels and chemicals by a variety of processes.[1–4] Capital and operating costs can be reduced by processing the biomass at high solids concentration.[5–7] Unfortunately, concentrated biomass is typically a complex fluid with a significant yield stress, which makes mixing, heating, and transporting challenging.[8,9] It is thus apparent that measuring, understanding, and controlling the rheological properties of biomass is essential for the development of economical processes. In this article, we describe a new, convenient method for measuring the yield stress of biomass, as well as that of other yield stress fluids.

Lignocellulosic biomass from woody plants, such as corn stover (corn stalks, leaves, cob, and husk), perennial grasses, and forest residues, are composed of cellulose, hemicellulose, and lignin. In processes designed to convert biomass to fuels and chemicals, the biomass is typically subjected to size reduction operations that produce fibrous particles. The resulting particle-size distribution can be quite broad, with maximum fiber lengths up to several centimeters. The particle size can be reduced further prior to thermal or chemical processing, but this adds additional processing costs. Fiber lengths and solids concentration then decrease further during the thermal and chemical processing steps.[10,11]

The rheological properties of biomass depend on the solids concentration as well as the fiber length distribution. Sufficiently dilute suspensions of fibers can behave as Newtonian fluids, whereas concentrated suspensions behave more like a paste with a substantial yield stress.[12–16] The concentration ranges defining these regimes depend on the fiber length.[17,18] The concentrated regime is of most interest for biomass processing, and the yield stress is the primary rheological parameter required for the design of processes and equipment.[15]

Measuring rheological properties of biomass can be challenging, especially when the particles are large or the concentration of insoluble solids is large. This has been illustrated in several recent studies in which a variety of measurement geometries and techniques were used.[14–16] Parallel disk geometries can be used provided that the particles are not too large and the suspension is not too concentrated. Phenomena that complicate or prohibit measurements at large concentrations include wall slip, edge fracture, and ejection. Knutsen and Liberatore[14] also showed that measured shear stress values depend on the normal load for concentrated systems, which makes it difficult to extract material properties.

Vane geometries can be used for concentration ranges similar to those accessible with parallel disk geometries,[15] and can accommodate larger particles. The main limitation is that, above some limiting concentration, the vane cannot be inserted into the sample without compressing the sample.[17] This limiting concentration decreases with increasing fiber length, and can be decreased by adding rheological modifiers.

A torque rheometer[19,20] can be used to measure apparent rheological properties of highly concentrated biomass suspensions.[16,21] The main limitations of this technique are that the method is time consuming, and the particle-size distribution can be reduced during the measurement. Nonetheless, Stickel et al.[15] showed that for an acid-hydrolyzed corn stover sample, yield stresses measured using torque rheometry at high-solids concentration were consistent with values obtained using parallel disk and vane geometries at smaller concentrations. The combined yield stress data were well-represented by the power-law expression

Correspondence concerning this article should be addressed to D. J. Klingenberg at klingen@engr.wisc.edu.

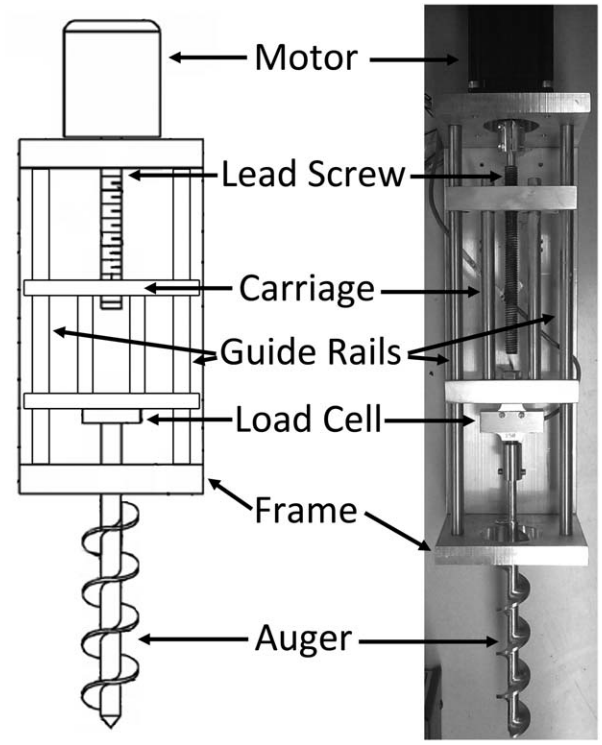

Figure 1. Schematic diagram and photograph of the "yield meter."

$$\tau_0 = a\,C_m{}^b \tag{1}$$

where τ_0 is the yield stress, C_m is the solid-mass fraction, and a and b are empirical parameters. Such a power-law dependence is commonly observed for natural fiber systems.[18,22]

Rheological parameters can also be estimated using a variety of "practical" rheological tests, such as the slump test, the squeeze test, and cone penetrometry.[23–25] These methods are rapid, inexpensive approaches for estimating parameters that correlate well with various operations or processes. We have found, however, that these methods do not work well for untreated biomass samples, because a variety of limitations discussed below prohibit the use of approximate analyses for extracting the shear yield stress. In the slump test, the continuous phase separates from the solid phase at small solids concentrations, and the material does not slump at large solids concentrations. In the squeeze test, the continuous phase again separates from the solid phase at small solids concentrations, and the biomass compresses at large solids concentrations. Cone penetrometry can be used at small solids concentrations, but the sample compresses at large solids concentrations.

In this article, we describe a new method for rapidly and inexpensively measuring the yield stress of concentrated biomass samples. The method uses an auger that is inserted into a sample much like a screw is inserted into a piece of wood. The auger is then translated axially while the axial force is measured. The maximum force measured at small translation rates divided by the cylindrical yield surface area is equated with the yield stress. Yield stress values obtained with this new "yield meter" compare well with values obtained using other techniques. We also show that this method can be used for yield stress materials other than biomass, and that other modes of operation, such as oscillatory shear, are possible.

Materials and Methods

Prototype design

A schematic diagram and a photograph of the yield meter are presented in Figure 1. The auger (Auger Fabrication, Exton, PA) has a flighted shaft that is 150-mm long, 25.4 mm in diameter, 3-mm thick, and has a pitch of 25.4 mm. The auger shaft diameter is 9 mm. The auger is attached to a load cell (LC703-150, 670 N maximum load, Omega Engineering, Stamford, CT) via a coupling with a set screw. The output from the load cell is recorded using LabView via a Cole-Parmer control box to a USB connection. The load cell is attached to a carriage that slides along guide rails, which allows the auger to be translated without rotating. The carriage is translated by a lead screw (1.5-mm pitch) attached to a stepper motor (G723-280-4, Geckodrive Motor Controls, Tustin, CA) and controller (Model G201X, Geckodrive Motor Controls, Tustin, CA). The motor is mounted to a rigid aluminum frame, is driven by a square-wave, 3.5-V peak-to-peak signal from a function generator, and has a maximum holding torque of 1.98 Nm and an encoder resolution of 2000 steps/revolution. The motor and carriage speeds are proportional to the frequency, f, of the input voltage, with the carriage speed in mm/s given by $7.94 \times 10^{-5} f$.

Measurement procedure

Before measurements are made, the weight of the attached auger is measured using the load cell with the auger hanging freely. The yield stress fluid is loaded into a 100-mm diameter, 150-mm long cylindrical container. The auger is then detached from the load cell by loosening the set screw and inserted ("drilled") into the sample material by rotating the auger by hand in a screw-like fashion (Figure 2a). This is a

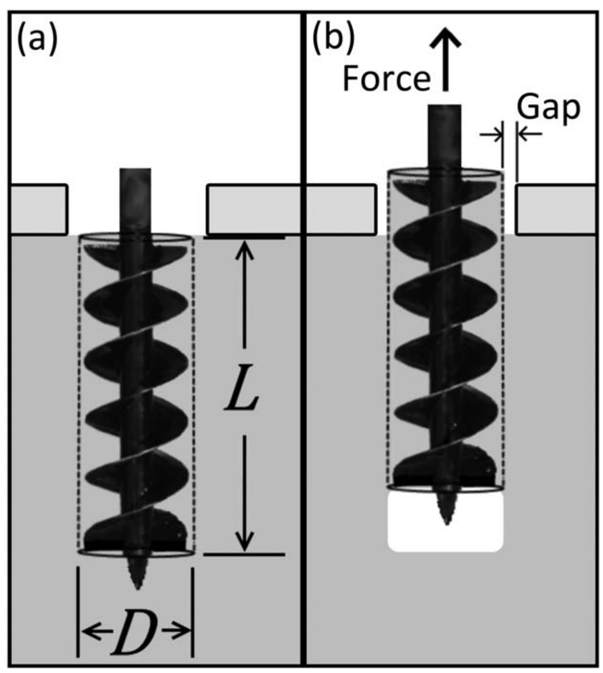

Figure 2. Schematic drawing of (a) the auger after insertion into a sample material but prior to operation and (b) the auger after it has been displaced during a measurement.

The depth of insertion, L, the auger diameter, D, and the gap between the auger and frame are indicated.

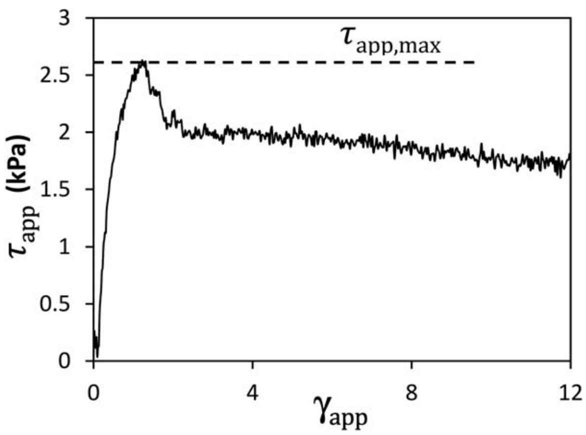

Figure 3. Example data for apparent shear stress as a function of apparent shear strain for a single yield meter run with Play-Doh at 22°C.

Apparent shear stress increases at small γ_{app} values, reaches a maximum, and then decreases with increasing γ_{app}.

critical step in the experimental procedure, and must be accomplished without significantly disturbing the fluid. The frame–motor–load cell assembly is then placed onto the auger such that the bottom of the frame is supported by the sample container. The auger is attached to the load cell by tightening the set screw.

Data from the load cell (force) is recorded at 5 Hz, beginning just before the motor is turned on. The motor is then used to drive the carriage, load cell, and auger at a predetermined speed. The force measured by the load cell increases as the auger begins to translate (without rotating). For all yield stress fluids examined, the material yields along the cylindrical surface defined by the auger flights, as illustrated in Figure 2b. Between measurements, the sample material is removed from the sample container, mixed, and reloaded. Measurements were made in triplicate and error bars in figures here represent a single standard deviation.

We assume that the contribution to force measurements from the complex material deformation near the end of the auger can be neglected. We also assume that the sample material deforms as a plug in such a way that the shear surface is coincident with the surface of the cylinder defined by the depth of insertion, L, and the auger diameter, D, as shown in Figure 2. The apparent shear stress can then be written as

$$\tau_{app} = \frac{F}{\pi DL} \quad (2)$$

where F is the force measured during deformation, indicated in Figure 2b.

The apparent stress depends on the deformation and rate of deformation. Apparent strain, γ_{app}, is defined as the axial displacement of the auger divided by the gap indicated in Figure 2b, and the apparent strain rate, $\dot{\gamma}_{app}$, is defined as the axial displacement rate divided by the gap. Example data for a "stress growth" measurement, in which τ_{app} is measured as a function of γ_{app}, is plotted in Figure 3. The apparent stress passes through a maximum, denoted by $\tau_{app,max}$. For sufficiently small shear rates, all materials investigated exhibit this maximum. We define the yield stress as

$$\tau_0 \equiv \lim_{\dot{\gamma}_{app} \to 0} \tau_{app,max} \quad (3)$$

Vane rheometry

Yield stress measurements made with the yield meter were compared with results obtained from a vane rheometer. The vane geometry is commonly used to obtain rheological properties for yield stress fluids.[14,26] The vane geometry used in this study consists of a four-bladed vane and a baffled cup. Yield stresses were obtained using the stress growth method whereby stress is measured at a constant shear rate and the maximum stress at low deformation rates is equated with the yield stress. An apparent shear rate of $0.0085\ s^{-1}$ was chosen because the maximum stress was not a function of shear rate below this value. Additional details of the device geometry and calibration can be found elsewhere.[27]

Materials

The yield meter was used to measure the yield stress of numerous colloidal, fibrous, and granular materials, listed in Table 1. Also listed in Table 1 is the type of suspension, and in most cases, an estimate of either the maximum particle size or the average particle size. Yield stresses of these materials were measured at 20°C unless otherwise specified.

Results and Discussion

Effect of apparent shear rate

The maximum apparent shear stress obtained using the yield meter, $\tau_{app,max}$, is plotted as a function of apparent shear rate for Play-Doh in Figure 4. For this material, $\tau_{app,max}$ is independent of shear rate below a shear rate of $0.25\ s^{-1}$. For other materials investigated, $\tau_{app,max}$ is independent of shear rate for shear rates less than $0.2\ s^{-1}$. Unless otherwise specified, all subsequent measurements were made at a shear rate of $0.05\ s^{-1}$, and $\tau_{app,max}$ measured at this shear rate was equated with the yield stress.

Effect of gap size

The yield stress is plotted as a function of the gap between the auger flights and the frame (see Figure 2b) for four different materials in Figure 5. For Play-Doh and soil,

Table 1. Particle-Size Information for the Materials Tested

Material	Suspension Type	Particle-Size Estimate
Play-Doh®	Colloidal	
Hydrolyzed hardwood fibers (HHWF)	Fibrous	<8 mm
Refined corn stover	Fibrous and granular	<3 mm
Joint compound	Colloidal	
Soil	Fine granular	<3.6 mm[a]
Mayonnaise	Colloidal	
Nylon	Fibrous	6.5 mm
Concrete	Coarse granular	<15 mm
Grease	Colloidal	
Sand	Fine granular	<420 μm[a]
Bleached aspen wood fibers	Fibrous	0.28 mm[b]
Wood flour	Fine granular	<208 μm[a]

[a]Indicates that the value represents the maximum particle size determined from shake-screen classification.
[b]Indicates that the value represents weighted average length.

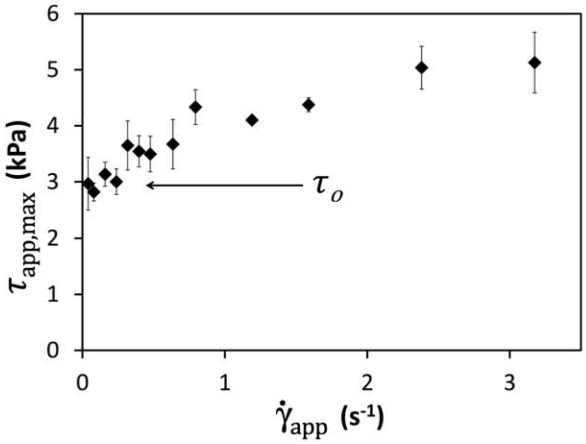

Figure 4. Maximum apparent shear stress as a function of $\dot{\gamma}_{app}$ for Play-Doh using the yield meter.

Below 0.25 s^{-1}, $\tau_{app,max}$ is independent of $\dot{\gamma}_{app}$.

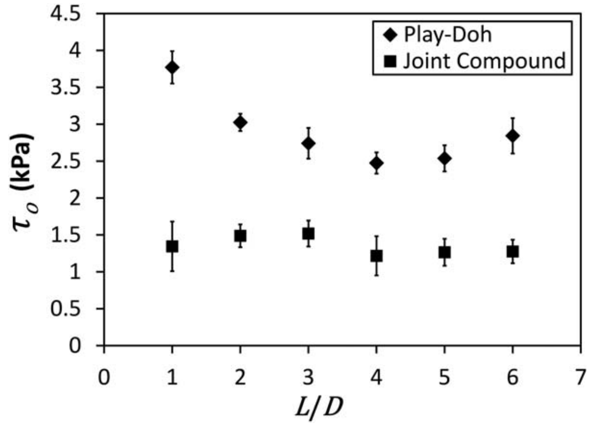

Figure 6. Yield stress as a function of depth of insertion (scaled by the gap, *D*) for Play-Doh and joint compound.

which have particle sizes smaller than the gap, the yield stress is independent of the gap over the range of gaps investigated here. For the Nylon fibers, the yield stress is independent of the gap for gap sizes greater than the fiber length (6.5 mm), but increases for gaps smaller than the fiber length. For concrete, the measured yield stress decreases with increasing gap over the entire range of gaps investigated. The largest particle size within the concrete is 15 mm, which is larger than the largest gap investigated (12.8 mm). From the results depicted in Figure 5, it is apparent that gap should be larger than the particle size to get results that are independent of the gap.

Effect of auger aspect ratio

The auger does not need to be inserted fully into the samples to measure a force when it is removed. The yield stress is plotted as a function of the depth of insertion, *L*, divided by the auger diameter, *D*, in Figure 6 for Play-Doh and joint compound. For the joint compound, the measured yield stress is independent of the depth of insertion. For Play-Doh, the yield stress increases with decreasing depth of insertion for values of L/D less than approximately 3. Such a dependence on the depth of insertion is expected to arise for sufficiently small depths as the stress acting on the end of the auger is ignored in the analysis. For these materials, the depth-to-diameter ratio should be $L/D > 3$ to obtain results that are independent of L/D.

Effect of cavitation

The process of extracting the auger can result in the formation a sample-free space, or cavity, at the end of the auger, as illustrated in Figure 2b. If air cannot enter this space, the reduced pressure would increase the force on the load cell and potentially produce erroneously large values of yield stress. To assess whether or not this phenomenon impacts the measured yield stress, set of experiments were performed in which the sample container was modified with a small hole that allows air to enter the sample below the auger. Yield stresses measured for three materials in the original sample container are compared with those measured using the modified container with the hole in the bottom in Figure 7. The yield stress values are the same for the two containers, and thus the space created below the auger when it is removed does not appear to influence the measured stresses.

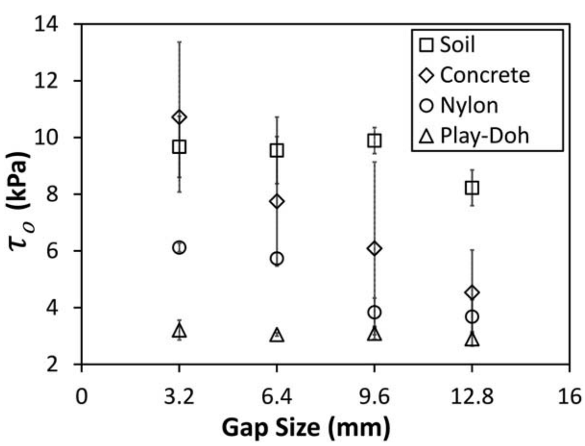

Figure 5. Yield Stress as a function of gap size for four different materials.

The gap is indicated in Fig. 2(b). Relevant measures of particle size for each material are shown in Table 1.

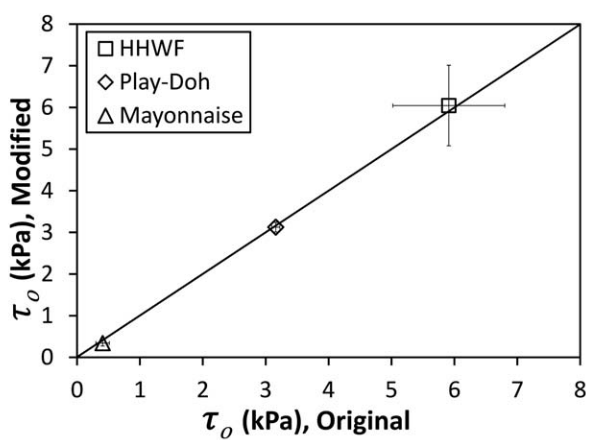

Figure 7. Comparison of yield stresses obtained using the original container and the modified container with the hole in the bottom, for three different samples.

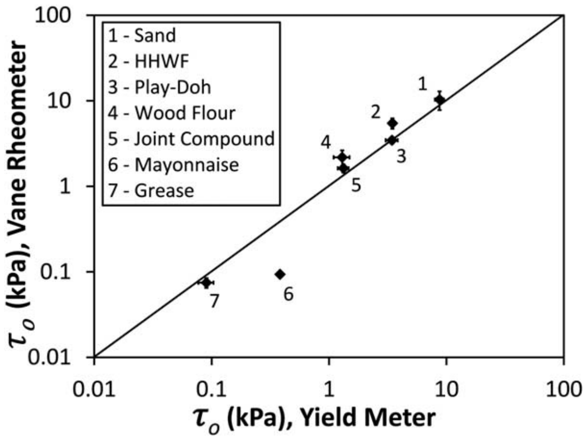

Figure 8. A comparison of τ_0 measurements made in the vane rheometer and the yield meter for different materials.

Comparison with the vane rheometer

In Figure 8, yield stress values obtained using the yield meter are compared with yield stress values obtained using the vane rheometer for several materials. Results obtained using the yield meter agree within experimental uncertainty for several of the materials tested, and differ by less than a factor of two for all materials except mayonnaise.

Yield stress of biomass

The yield meter is capable of measuring the yield stress of concentrated lignocellulosic biomass suspensions. Figure 9 shows the yield stress as a function of solids concentration for suspensions of bleached aspen wood fibers. The fibers were prepared by exposing pressure-refined aspen wood chips to a chloro-acetate bleaching process.[28] The rapid increase of yield stress with increasing solids concentration in Figure 9 is consistent with results from many rheological studies of lignocellulosic biomass.[13,15,16,22,29] A fit of Eq. 1 to the data results in a value of parameter b of 1.8 ± 0.6.

The yield stress of untreated, refined corn stover is plotted as a function of solids concentration in Figure 10. Data obtained using the yield meter are plotted along with data obtained using the vane geometry. Above 20 wt % solids, the vane rheometer could not be used because the vane could not be inserted into the sample. Measurements were made with the yield meter up to 57 wt % solids (the corn stover was acquired at this solids concentration). For concentrations where both techniques can be used, $C_m \leq 20$ wt %, the yield stresses from the two techniques are similar. Below 35 wt % solids, the data obtained using the yield meter follows the power-law relationship of Eq. 1. A fit of Eq. 1 to this data results in a value of b of 3.6 ± 0.1, which is in agreement with results for other refined biomass.[18,22] At solids concentrations of 45 and 57 wt %, the refined corn stover contained entrained air and became highly compressible. As a result, the bulk density was smaller than that at lower solids concentration, and not easily controlled. These samples are indicated by the filled symbols in Figure 10.

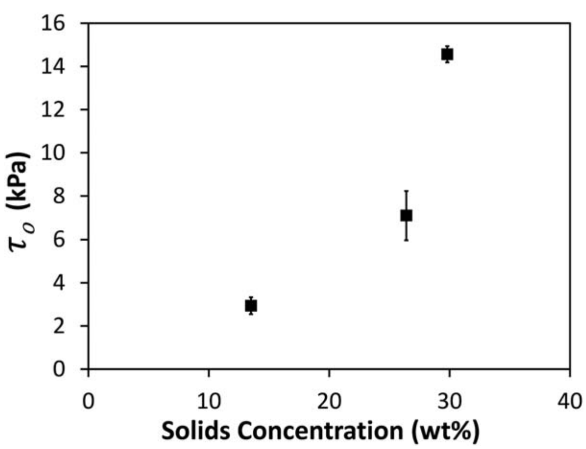

Figure 9. Yield stress as a function of solids concentration measured in a suspension of bleached aspen wood fibers.

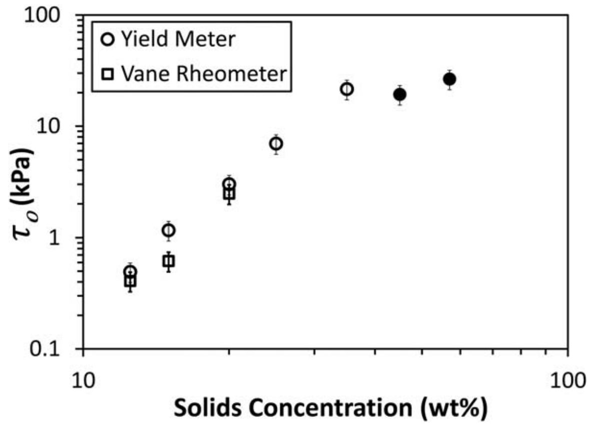

Figure 10. Yield stress of refined corn stover vs. solids concentration.

Measurements were made using the vane rheometer and the yield meter. The vane rheometer could not be used to make measurements above 20 wt % solids. The filled symbols (45 and 57 wt % solids) indicate that air was entrained in the sample and the bulk density was smaller than that at lower solids concentrations. Error bars indicate 20% uncertainty, the value of a single standard deviation based on triplicate measurements at 20 wt % solids.

Oscillatory mode

The procedure used for all measurements in this study requires deformation of the sample beyond the regime where stress depends linearly on strain so that $\tau_{app,max}$ can be obtained. Prior to the next measurement, the auger must be removed and the sample must be mixed. The yield meter may also be operated by translating the auger in an oscillatory manner to obtain dynamic stress–strain data. Dynamic properties, that is, G' and G'',[30] may be obtained if the deformation remains in the linear regime. It may also be possible to relate dynamic mechanical properties, for example, elastic modulus, to other rheological properties of interest such as the yield stress.[31,32] This approach would make it easier to measure time-dependent rheological properties.

Conclusions

A method for measuring yield stress that utilizes an auger to deform a sample was developed and tested. The technique avoids difficulties encountered with conventional rheometric techniques, such as wall slip, sample disruption during preparation, high normal stresses, and phase separation. It can be used with a wide range of industrially relevant yield stress fluids including concentrated lignocellulosic biomass, concrete, and food products. The effects of strain rate, gap size, and auger aspect ratio were examined. Results from the yield meter compared well with results obtained using a vane rheometer. The device may also be used in oscillatory mode, which would make it easier to measure time-dependent rheological properties.

Acknowledgment

This project was supported by the U.S. Department of Agriculture (NRI award number 2006-35504-17401 and AFRI award number 2010-65504-20406).

Literature Cited

1. Serrano-Ruiz JC, Wang D, Dumesic JA. Cataytic upgrading of levulinic acid to 5-nonanone. *Green Chem.* 2010;12:574–577.
2. Aden A, Ruth M, Ibsen K, Jechura J, Neeves K, Sheehan J, Wallace B, Montague L, Slayton A, Lukas J. Lignocellulosic biomass to ethanol process design and economics utilizing co-current dilute acid prehydrolysis and enzymatic hydrolysis for corn stover: NREL, *Report No.* TP-510–32438, 2002.
3. Bozell JJ, Moens L, Elliott DC. Production of levulinic acid and use as a platform chemical for derived products. *Resour Conserv Recycl.* 2000;28:227–239.
4. Serrano-Ruiz JC, Braden DJ, West RM, Dumesic JA. Conversion of cellulose to hydrocarbon fuels by progressive removal of oxygen. *Appl Catal B Environ.* 2010;100:184–189.
5. Jorgensen H, Kristensen JB, Felby C. Enzymatic conversion of lignocellulose into fermentable sugars: Challenges and opportunities. *Biofuels Bioprod Biorefining.* 2007;1:119–134.
6. Wingren A, Galbe M, Zacchi G. Techno-economic evaluation of producing ethanol from softwood: comparison of SSF and SHF and identification of bottlenecks. *Biotechnol Progr.* 2003;19(4):1109–1117.
7. Lynd LR, Elander RT, Wyman CE. Likely features and costs of mature biomass ethanol technology. *Appl Biochem Biotechnol.* 1996; 57–58:741–761.
8. Rosgaard L, Andric P, Dam-Johansen K, Pedersen S, Meyer AS. Effects of substrate loading on enzymatic hydrolysis and viscosity of pretreated barley straw. *Appl Biochem Biotechnol.* 2007;143:27–40.
9. Um B-H, Hanley TR. High-solid enzymatic hydrolysis and fermentation of Solka Floc into ethanol. *J Microbiol Biotechnol.* 2008;18: 1257–1265.
10. Samaniuk JR, Scott CT, Root TW, Klingenberg DJ. The effect of high intensity mixing on the enzymatic hydrolysis of concentrated cellulose fiber suspensions. *Bioresour Technol.* 2011;102:4489–4494.
11. Roche CM, Dibble CJ, Knutsen JS, Stickel JJ, Liberatore MW. Particle concentration and yield stress of biomass slurries during enzymatic hydrolysis at high-solids loadings. *Biotechnol Bioeng.* 2009; 104(2):290–300.
12. Pimenova NV, Hanley TR. Measurement of rheological properties of corn stover suspensions. *Appl Biochem Biotechnol.* 2003;105:383–392.
13. Pimenova NV, Hanley TR. Effect of corn stover concentration on rheological characteristics. *Appl Biochem Biotechnol.* 2004;113:347–360.
14. Knutsen JS, Liberatore MW. Rheology of high-solids biomass slurries for biorefinery applications. *J Rheol.* 2009;53(4):877–892.
15. Stickel JJ, Knutsen JS, Liberatore MW, Luu W, Bousfield DW, Klingenberg DJ, Scott CT, Root TW, Ehrhardt MR, Monz TO. Rheology measurements of a biomass slurry: an inter-laboratory study. *Rheol Acta.* 2009;48(9):1005–1015.
16. Ehrhardt MR, Monz TO, Root TW, Connelly RK, Scott CT, Klingenberg DJ. Rheology of dilute acid hydrolyzed corn stover at high solids concentration. *Appl Biochem Biotechnol.* 2010;160(4): 1102–1115.
17. Samaniuk JR, Wang J, Root TW, Scott CT, Klingenberg DJ. Rheology of concentrated biomass. *Korea-Aust Rheol J.* 2011;23(4):237–245.
18. Kerekes RJ. Rheology of suspensions:—rheology of fibre suspensions in papermaking: an overview of recent research. *Nord Pulp Pap Res J.* 2006;21(5):598–612.
19. Blyler LL, Daane JH. An analysis of Brabender torque rheometer data. *Polym Eng Sci.* 1967;7(3):178–181.
20. Goodrich J, Porter R. A rheological interpretation of torque-rheometer data. *Polym Eng Sci.* 1967;7:45–51.
21. Samaniuk JR, Scott TC, Root TW, Klingenberg DJ. Rheological modification of biomass at high solids concentrations. *J Rheol.* 2011; 56:649–665.
22. Bennington CPJ, Kerekes RJ, Grace JR. The yield stress of fiber suspensions. *Can J Chem Eng.* 1990;68(5):748–757.
23. Pashias N, Boger DV, Summers J, Glenister DJ. A fifty cent rheometer for yield stress measurement. *J Rheol.* 1996;40(6):1179–1189.
24. Wright AJ, Scanlon MG, Hartel RW, Marangoni AG. Rheological properties of milkfat and butter. *J Food Sci.* 2001;66(8):1056–1071.
25. Roussel N, Coussot P. "Fifty-cent rheometer" for yield stress measurements: from slump to spreading flow. *J Rheol.* 2005;49:705–718.
26. Nguyen QD, Boger DV. Measuring the flow properties of yield stress fluids. *Annu Rev Fluid Mech.* 1992;24:47–88.
27. Monz TO. Investigation of biomass rheology in different geometries. Deplomarbeit Nr. 727, Stuttgart, Germany, 2007.
28. Moore WE, Johnson DB, editors. The chlorite-acetic acid method. In: *Procedures for the Checmical Analysis of Wood and Wood Products*. Madison, WI: USDA Forest Products Laboratory; 1967: 6–8.
29. Kerekes RJ, Soszynski RM, Tam Doo PA. *The Focculation of Pulp Fibers in Papermaking Raw Materials*. London: Mechanical Engineering Publications, 1985.
30. Bird RB, Armstrong RC, Hassager O. *Dynamics of Polymeric Liquids*, *Vol 1. Fluid Mechanics*, 2nd ed. New York: Wiley, 1987.
31. Chateau X, Ovarlez G, Trung KL. Homogenization approach to the behavior of suspensions of noncolloidal particles in yield stress fluids. *J Rheol.* 2008;52(2):489–506.
32. Mahaut F, Chateau X, Coussot P, Ovarlez G. Yield stress and elastic modulus of suspensions of noncolloidal particles in yield stress fluids. *J Rheol.* 2008;52(1):287–313.

Manuscript received Oct. 5, 2013, and final revision received Dec. 18, 2013.